AEROCLOUD

by

NABLAFLOW

CFD report

Showcase_car

Contents

Introduction

Thank you for using AeroCloud by NablaFlow. Our goal is to make advanced CFD-simulations fast and available to everyone. By keeping the workflow simple and efficient, we take care of the simulations while you can focus on design and development. The meshing and simulation processes are fully automated and tested on a wide range of validation cases to provide stable and reliable results.
This document summarizes the setup and results of a numerical aerodynamics study run on AeroCloud. The presented results are calcluated from the time averaged flow field and shown as global parameters and detailed spatial velocity and pressure field presentations. We try to use common conventions and definitions from the aerodynamics community, but these may vary between spesfic applications and fields. All definitions used here are described in the report.
The simulation result webpage can be accessed by scanning qr-code below.

Disclaimer

The simulations executed with AeroCloud follow the best practices for CFD simulations. However, simulations will always involve modelling, discretization and iteration errors. Therefore, we highly recomend that final designs and safety critical dimensioning parameters are verfied in wind tunnel experiments. We, at NablaFlow, collaborate with a large number of wind tunnel operators. To find a wind tunnel institute suited for your project, please contact us at info@nablaflow.io. NablaFlow is not responsible for the misuse of the information included in the present report.

Test case

Test details

Project	-
Test case	Showcase_car
Test date	2023-08-31
Number of parts	6
Units	Sports_Car_Parts_3.obj: m
Frontal area	1.8028 m^2
Surface area	36.2030 m^2

Simulation settings

Aerocloud version	v6
Simulation type	Standard
Fluid	Air
Kinematic viscosity	15.0 cSt
Density	1.225 kg/m^3
Speed	30.0 m/s
Yaw angles	0.0°, 5.0°
Ground	On
Rotation	Front_Wheels: rolling Rear_Wheels: rolling
Number of cells	11918870

3D-model

The uploaded 3D model has a projected frontal area of 1.803 m^2 and a total surface area of 36.203 m^2. The maximum extent of the model along the x, y and z axes is 3.767 m, 2.091 m and 1.023 m.

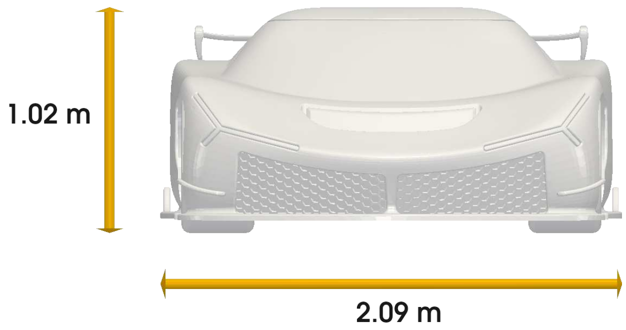

Figure 1: 3D model front view

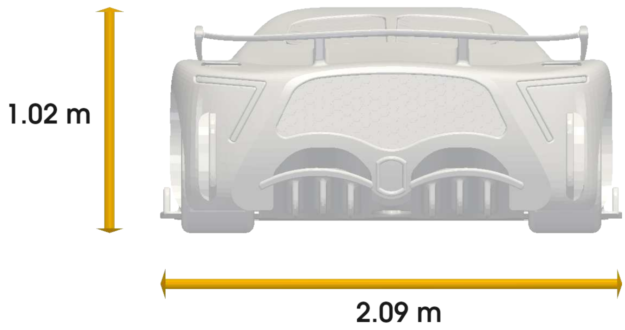

Figure 2: 3D model back view

Figure 3: 3D model left view

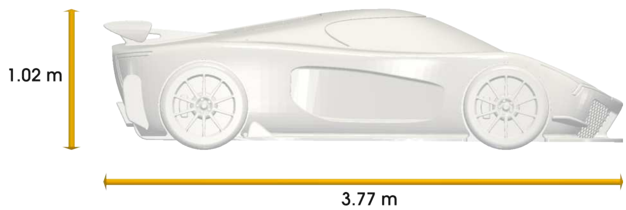

Figure 4: 3D model right view

Definitions

Coordinate system

Forces and moments are defined according to the right hand coordinate system shown in figure 5. The original coordinate system of the 3D-model(s) is adopted, with positive drag force along the x-axis and positive lift force along the z- axis.
Roll, pitch and yaw moments are calculated around the corresponding coordinate axes. The yaw angle is defined as the angle between the wind vector and the model x-axis and is positive counter-clockwise.

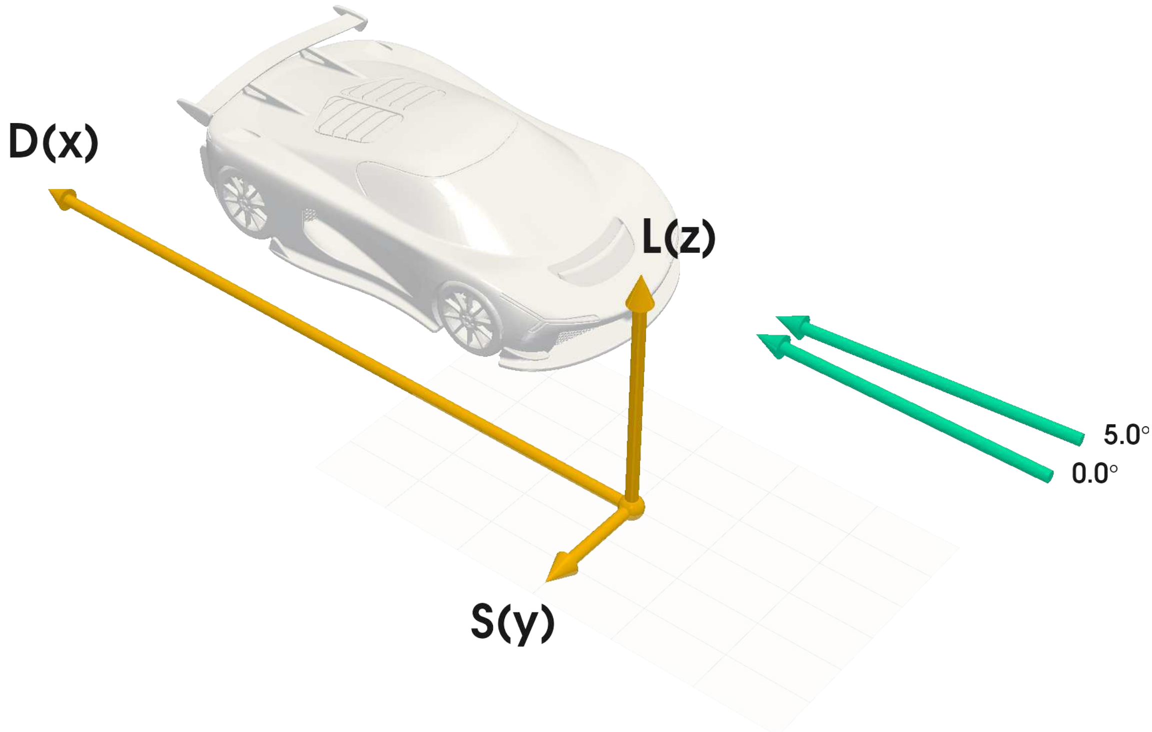

Figure 5: Coordinate system and wind direction

Nomenclature

Symbols		Subscripts	
A	Projected frontal area	d	Drag
C	Coefficient	l	Lift
F	Force	p	Pitch
L	Length scale	r	Roll
M	Moment	s	Side
P	Pressure	t	Total
U	Wind speed	w	Wall
μ	Dynamic viscosity	y	Yaw
ρ	Fluid density	∞	Freestream

Pressure

The total pressure field shows the energy in the flow around an object. The total pressure (P_t) is defined as the sum of the static pressure (P_{static}) and the dynamic pressure ($½\rho|u|^2$). Some of that energy will be dissipated into heat as an object is moving relative to a viscous fluid. When the boundary layer separates from an object, a low pressure, turbulent wake will form behind the object, and the resulting pressure difference around the object causes pressure drag. The velocity vector fields are visualized in the pressure plots in the report, by a technique called line integral convolution (LIC). This provides an intuitive visual impression of the flow direction of the decomposed velocity field on the projected plane.

The surface pressure shows the force per area normal to the surface of the body. The surface pressure decomposed along the three coordinate axes and integrated around the surface, gives drag, lift and side pressure force. The surface pressure is highest at the stagnation points, where the velocity is zero, and all the kinetic energy is coverted to pressure energy.

Wall shear stress

Shear stress in a fluid is a viscous stress component that excerts a force parallel to the local flow direction due to a normal velocity gradient. The shear stress on a solid boundary is called wall shear stress, and can be interperated as a frictional force which is directed along the local flow direction, tangential to the surface of the body. It is caused by the velocity gradient in the boundary layer next to the surface and fluid viscosity. This causes a drag force on the surface in the direction of the local flow. Areas of low wall shear stress has a low local flow velocity. Along separation lines the wall shear stress is zero.

$$\tau = \frac{F}{A} \qquad \tau_w = \mu \frac{\delta u}{\delta y}{}_{y=0}$$

Forces

Fluid dynamic forces on an object are the sum of pressure forces and viscous forces. In the results section, these forces are shown both individually and combined. Pressure forces are dominating for high Reynolds number flows around bluff bodies, while vicous forces are dominating for streamlined bodies and low reynolds numbers. Forces are calculated along each of the coordinate axes, fixed to the model.
Moments are calculated around each coordinate axes. The original coordinate system of the model is used to calculate the moments of all parts. Moments around each of the drag, lift and side force axes are denoted "roll" (r), "yaw" (y) and "pitch" (p) respectively.

Normalizations

Non-dimensional force- and moment coefficients are calculated by normalizing the aerodynamic force (F) and moment (M) components by the freestream dynamic pressure and predefined length scales. The reference area "A" is the projected frontal area and the reference length "L" is 1 meter.

$$C_F = \frac{F}{½\rho_\infty U_\infty^2 A} \qquad C_M = \frac{M}{½\rho_\infty U_\infty^2 AL}$$

Non-dimensional static- and total pressure coefficients are calculated by normalizing the static and total pressure by the freestream dynamic pressure.

$$C_{Pt} = \frac{P_{static} + ½\rho|u|^2}{½\rho_\infty U_\infty{}^2} \qquad C_P = \frac{P_{static}}{½\rho_\infty U_\infty{}^2}$$

A standard fluid density ρ = 1.225 is used for all normalizations. The freestream wind speed (U=30.0 m/s) is used for normalization for all yaw angles, implying that the model aligned wind will decrease for increasing yaw angle.

Drag surface

The drag pressure surface visualizes the local drag force density on the surface of a body in units of drag force per area. It is composed of the sum of the drag axis component of the local surface pressure vector and the drag axis component of the wall shear stress vector, and hence includes both the pressure drag and friciton drag contributions. The purpose of this plot is to indentify regions of the body where drag force is generated.

Streamlines

Streamlines show the trajectory of a fluid particle as it moves downstream in a fluid flow. They can be used to show the overall structure of the flow field around a body and the extent of the wake. To visualize the streamlines we add an seeding array of weightless particles into the flow upstream of the object, like smoke traces are used to visualize airflow in a wind tunnel. In areas of accelerated flow, the streamlines come closer to each other and in decelerated regions they will separate. The colors of the streamlines coresponds to the total flow velocity.

Recirculation zones

As flow separation occurs, regions of low pressure are formed downstream. In this region recirculating vortices are formed. These low pressure zones on the leeward side of a body causes a suction contributing to the drag force. The colored regions in the resirculation figures indicate volumes of a negative x-axis velocity component.

Results

The overall results are summarized in 1, 2, 3 and 4. Yaw-angle dependency of forces and moments are presented graphically below. Details of the flow field and forces per part for each individual CFD-simulation are presented in the following subchapters.

Forces and moments

Table 1: Aerodynamic forces and moments on model coordinate system

Yaw [°]	F_d [N]	F_s [N]	F_l [N]	M_r [Nm]	M_p [Nm]	M_y [Nm]
0.0	300.53	8.45	-315.35	457.72	435.70	477.77
5.0	309.30	167.61	-375.02	523.03	672.25	949.89

Force- and moment coefficients

Table 2: Aerodynamic force and moment coefficients on model coordinate system

Yaw [°]	C_d [-]	C_s [-]	C_l [-]	C_r [-]	C_p [-]	C_y [-]
0.0	0.302	0.009	-0.317	0.461	0.438	0.481
5.0	0.311	0.169	-0.377	0.526	0.676	0.956

Force-area

Table 3: Aerodynamic force coefficient x frontal area along model coordinate axes

Yaw [°]	C_dA [m^2]	C_sA [m^2]	C_lA [m^2]
0.0	0.545	0.015	-0.572
5.0	0.561	0.304	-0.680

Pressure- and viscous forces

Table 4: Pressure forces and viscous forces on model coordinate system

	Pressure force			Viscous force		
Yaw [°]	F_d [N]	F_s [N]	F_l [N]	F_d [N]	F_s [N]	F_l [N]
0.0	277.54	8.34	-319.38	22.99	0.11	4.02
5.0	286.47	164.79	-379.20	22.83	2.83	4.17

Yaw dependency

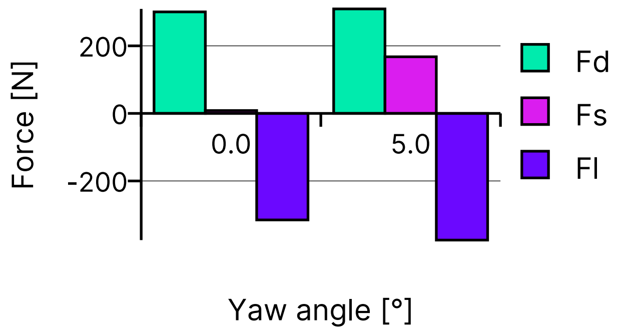

Figure 6: Net aerodynamic forces

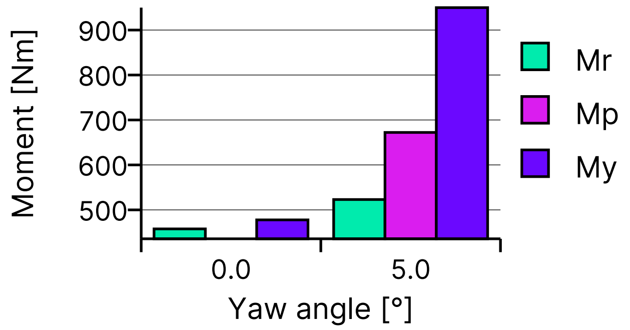

Figure 7: Net aerodynamic moments

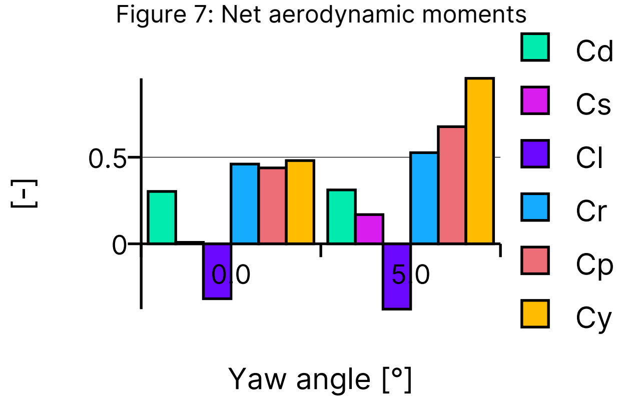

Figure 8: Aerodynamic force- and moment coefficents

Simulation details Yaw-angle = 0.0°

Streamlines

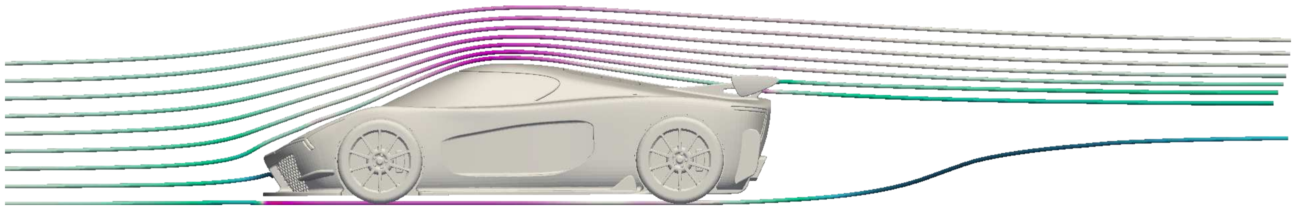

Figure 9: Streamlines left view

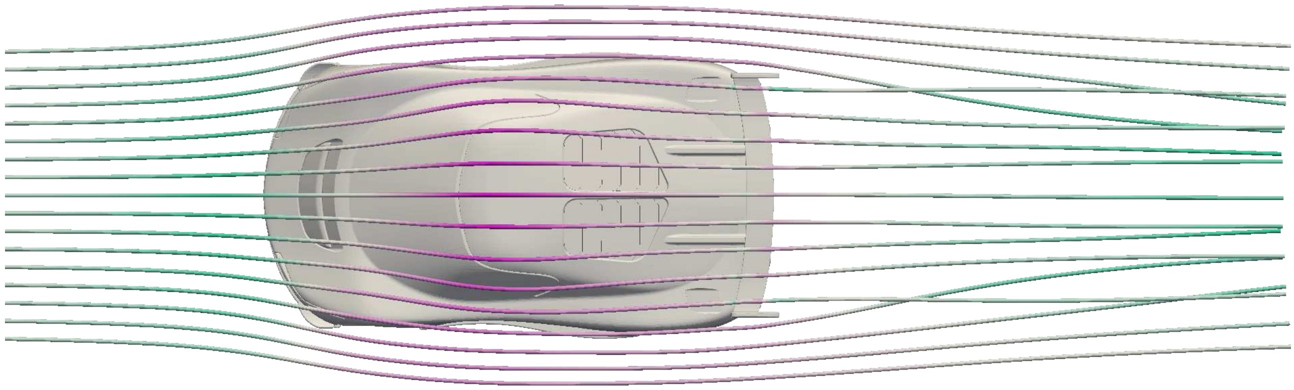

Figure 10: Streamlines top view

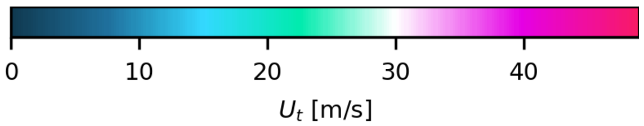

Pressure field

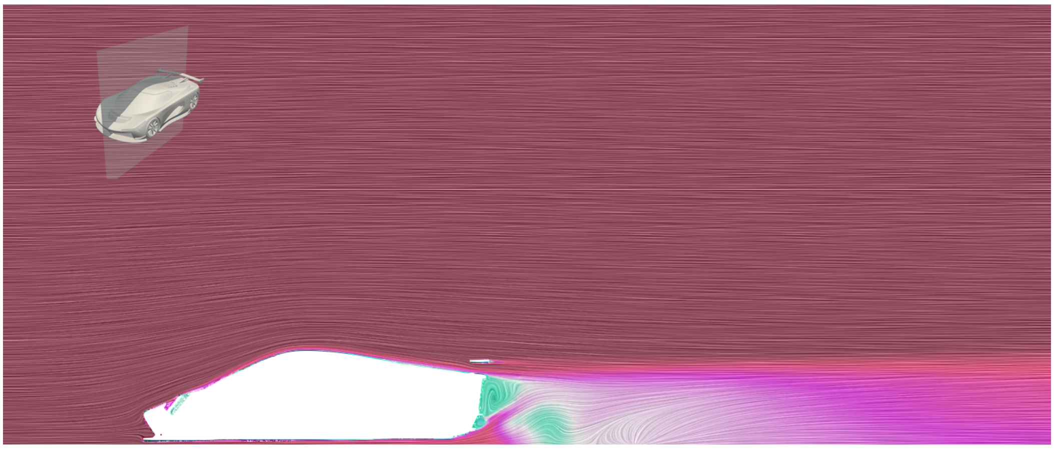

Figure 11: C_{pt} Total pressure coefficient in model centre XZ-plane

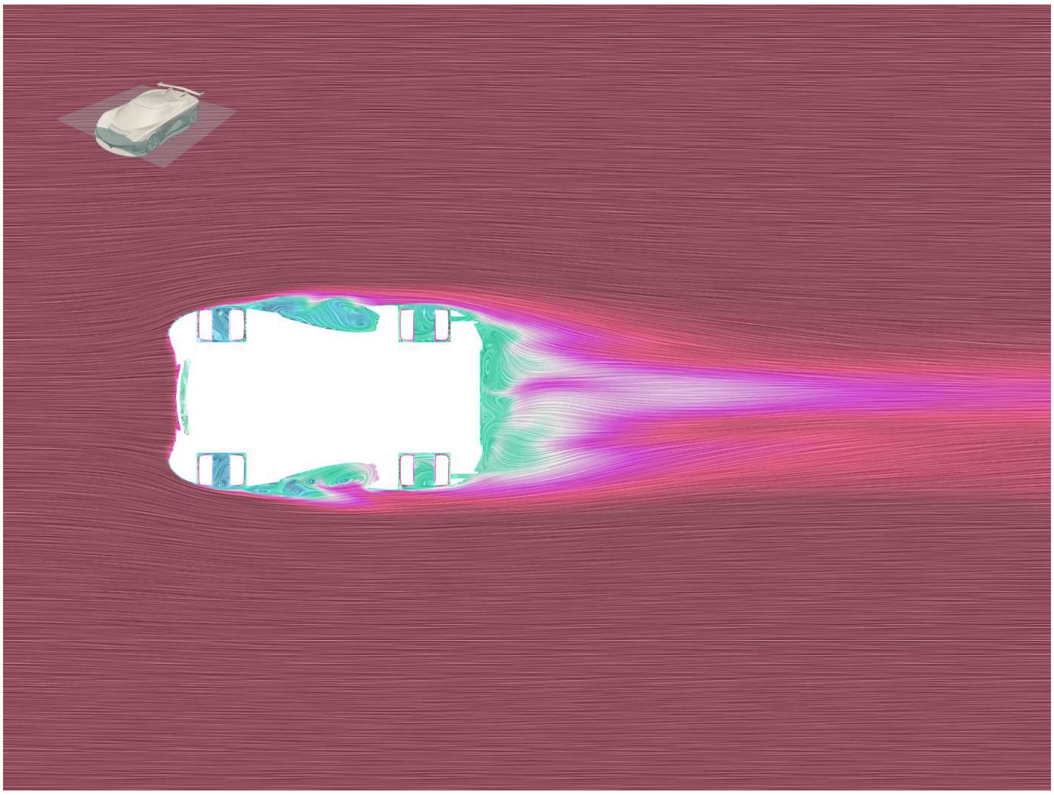

Figure 12: C_{pt} Total pressure coefficient in model centre XY-plane

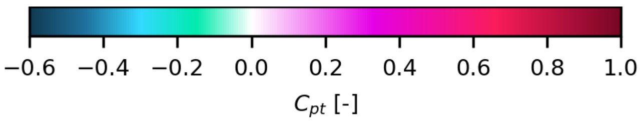

Surface pressure

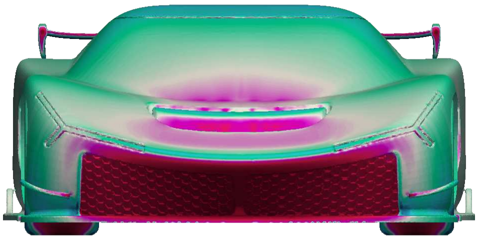

Figure 13: Surface pressure front view

Figure 14: Surface pressure back view

Figure 15: Surface pressure left view

Figure 16: Surface pressure right view

Figure 17: Surface pressure top view

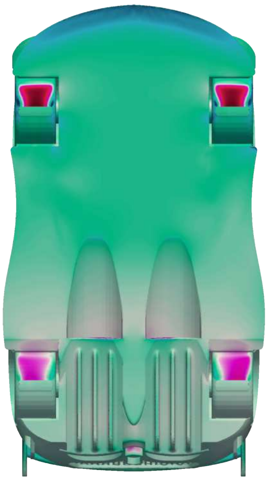

Figure 18: Surface pressure bottom view

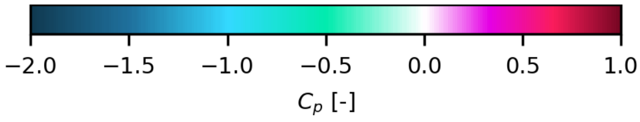

Wall shear stress

Figure 19: Wall shear stress front view

Figure 20: Wall shear stress back view

Figure 21: Wall shear stress left view

Figure 22: Wall shear stress right view

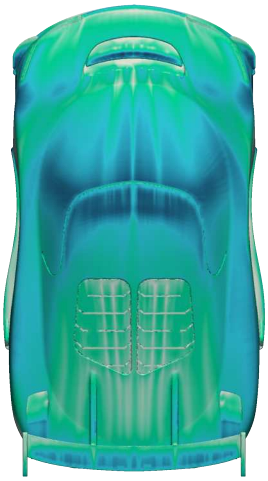

Figure 23: Wall shear stress top view

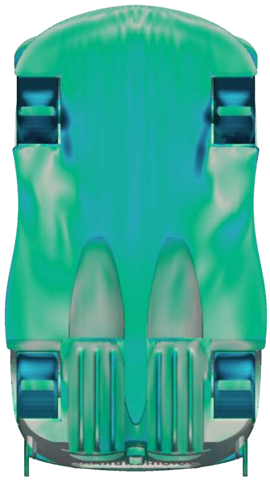

Figure 24: Wall shear stress bottom view

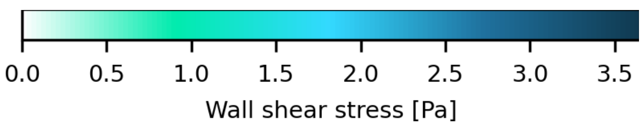

Drag pressure

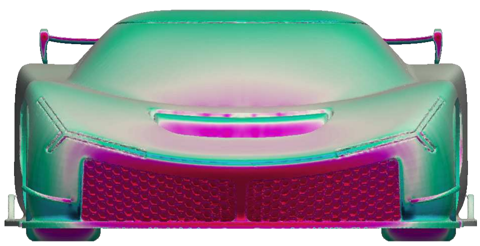

Figure 25: Drag pressure front view

Figure 26: Drag pressure back view

Figure 27: Drag pressure left view

Figure 28: Drag pressure right view

Figure 29: Drag pressure top view

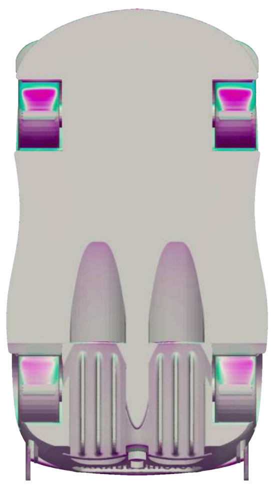

Figure 30: Drag pressure bottom view

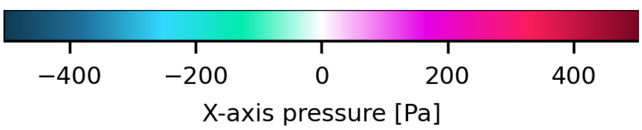

Recirculation zones

Figure 31: Recirculation zones front view

Figure 32: Recirculation zones back view

Figure 33: Recirculation zones left view

Figure 34: Recirculation zones right view

Figure 35: Recirculation zones top view

Figure 36: Recirculation zones bottom view

Wake development

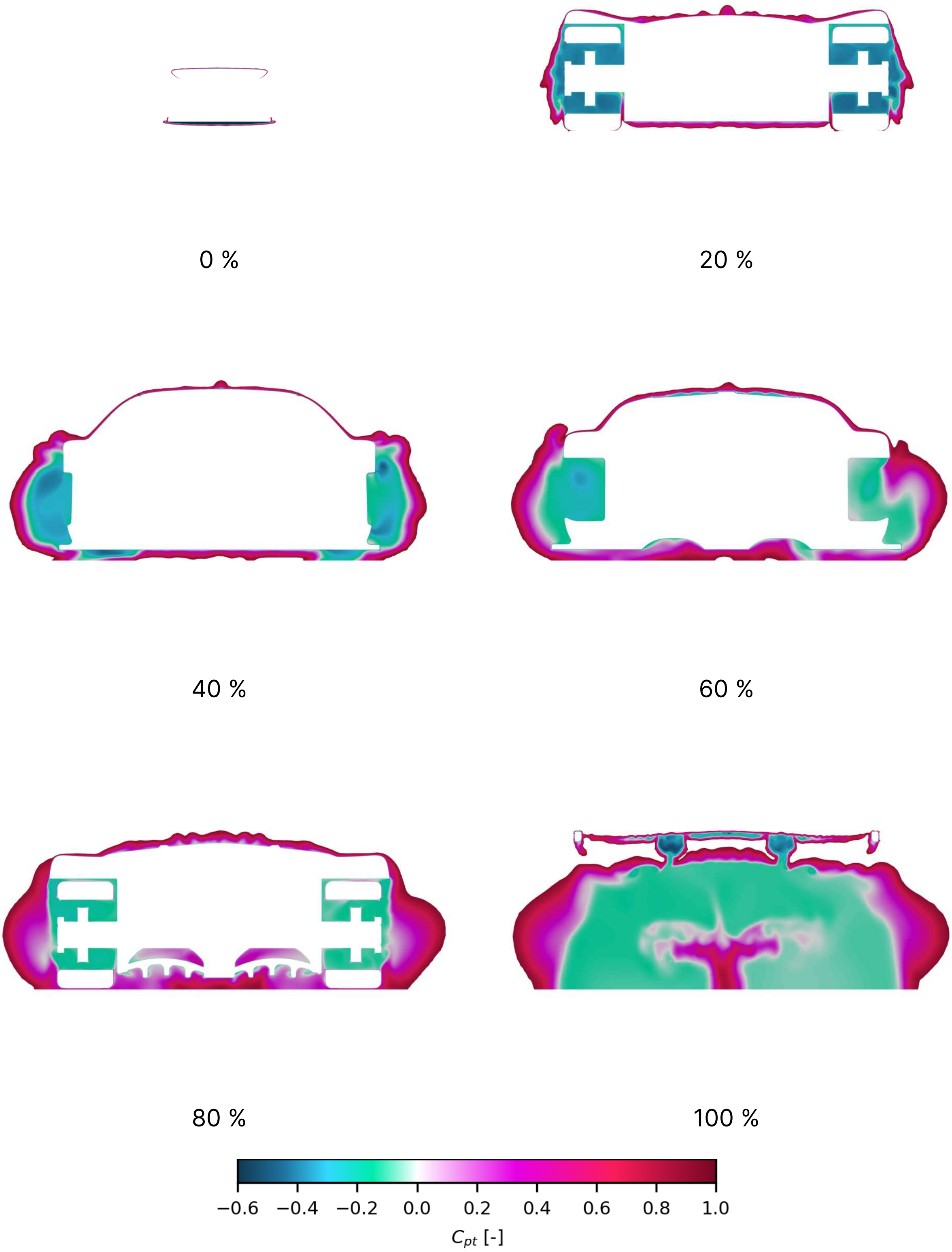

Figure 37: Wake development in the x-direction

Force distribution x-axis

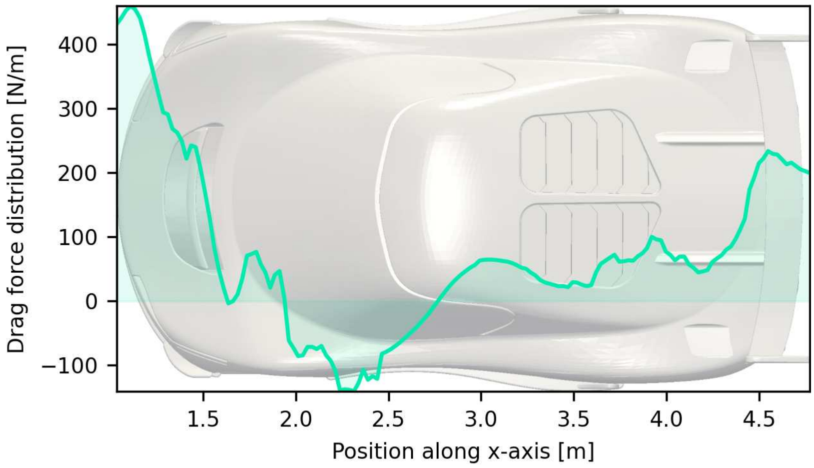

Figure 38: Drag force along x-axis

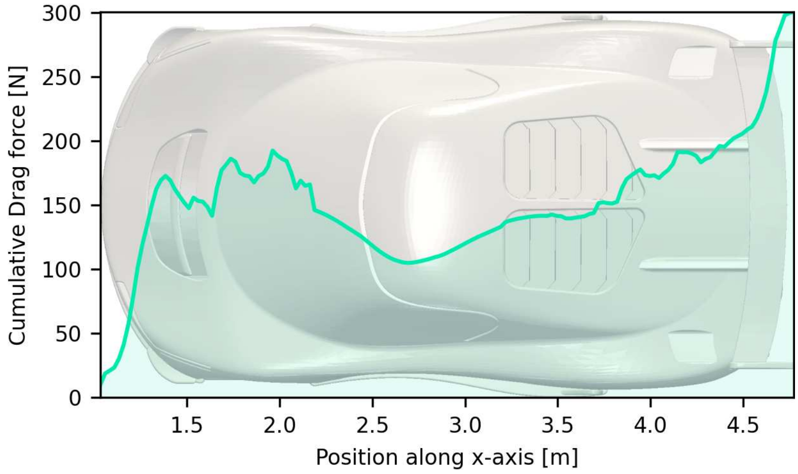

Figure 39: Cumulative drag force along x-axis

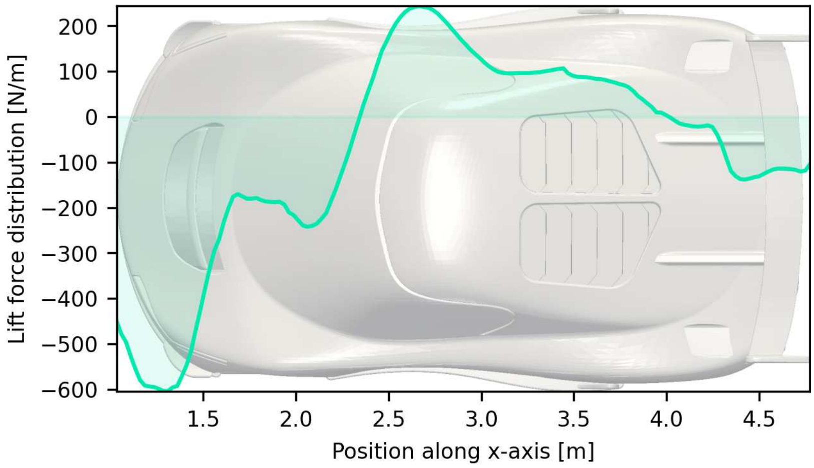

Figure 40: Lift force along x-axis

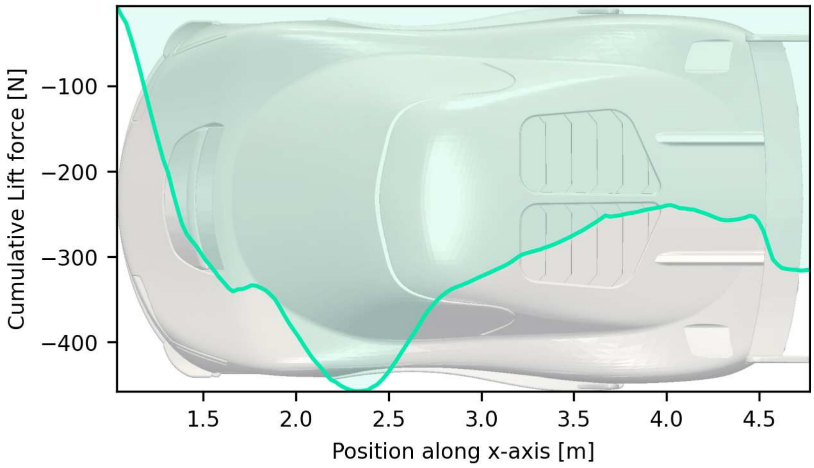

Figure 41: Cumulative lift force along x-axis

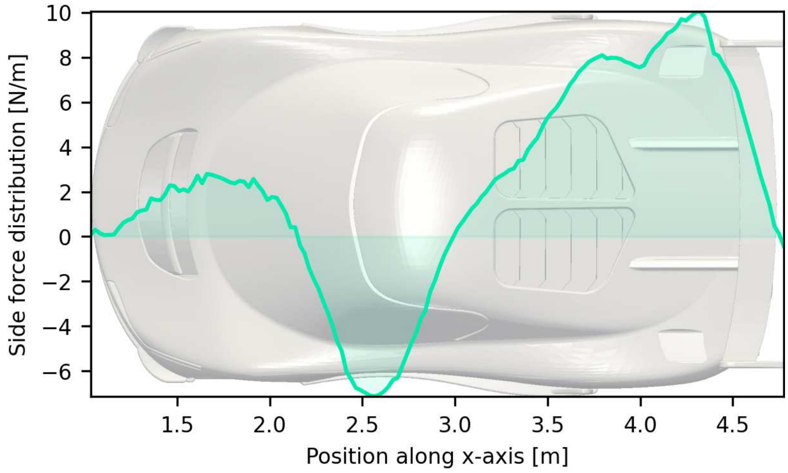

Figure 42: Side force along x-axis

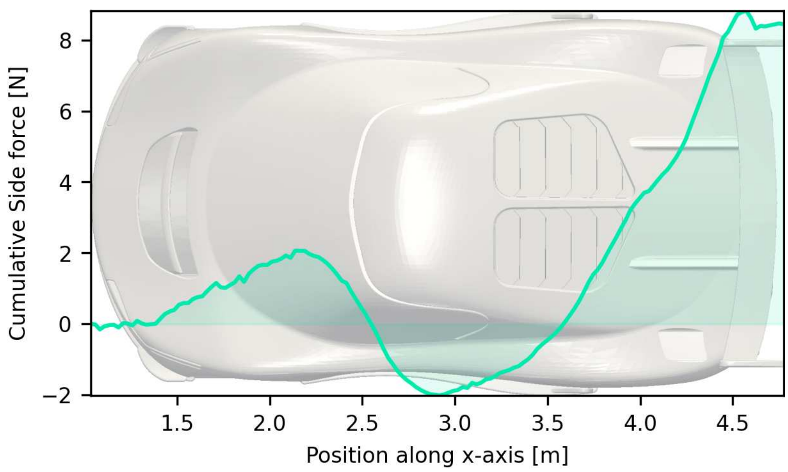

Figure 43: Cumulative side force along x-axis

Force distribution y-axis

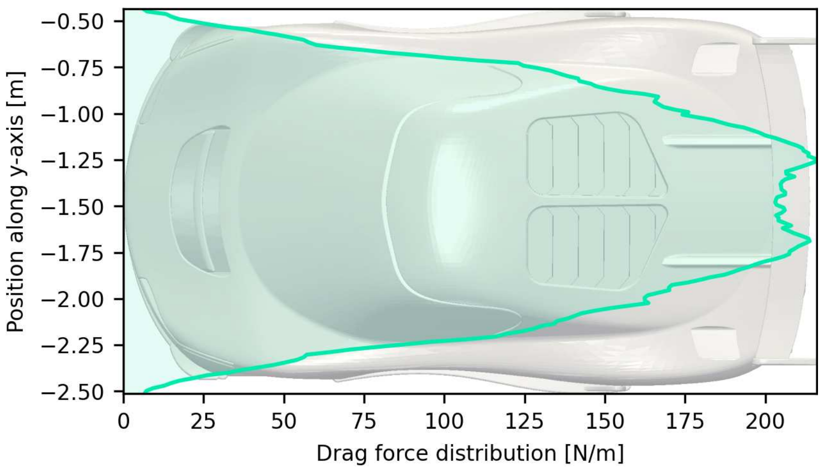

Figure 44: Drag force along y-axis

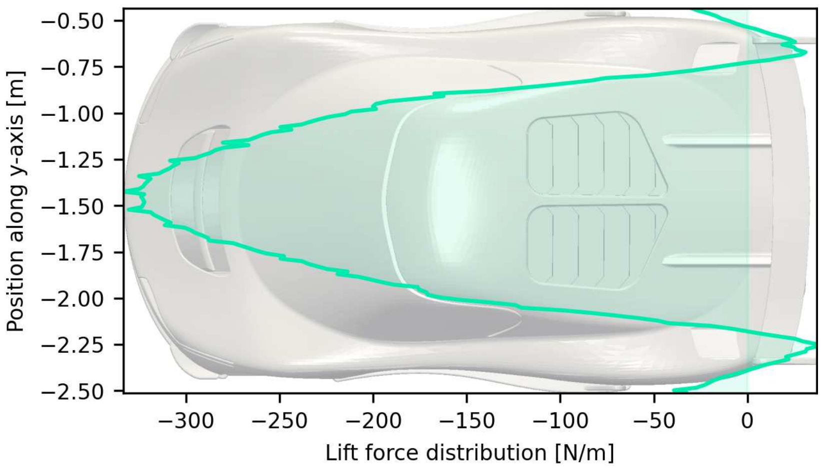

Figure 45: Lift force along y-axis

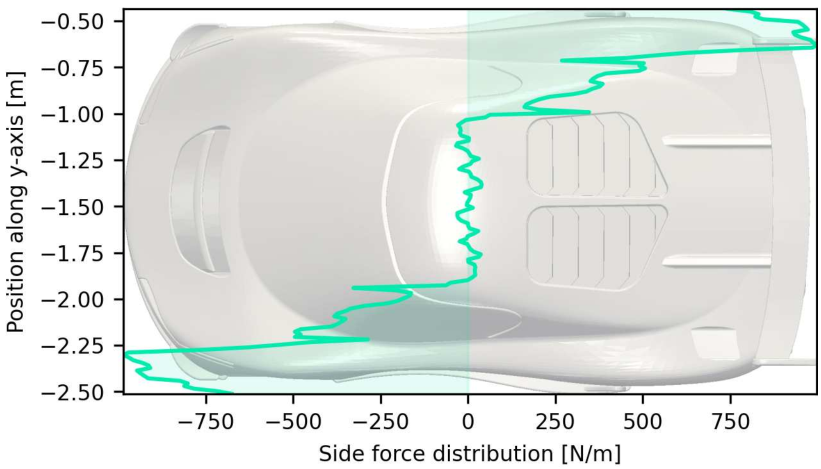

Figure 46: Side force along y-axis

Force distribution z-axis

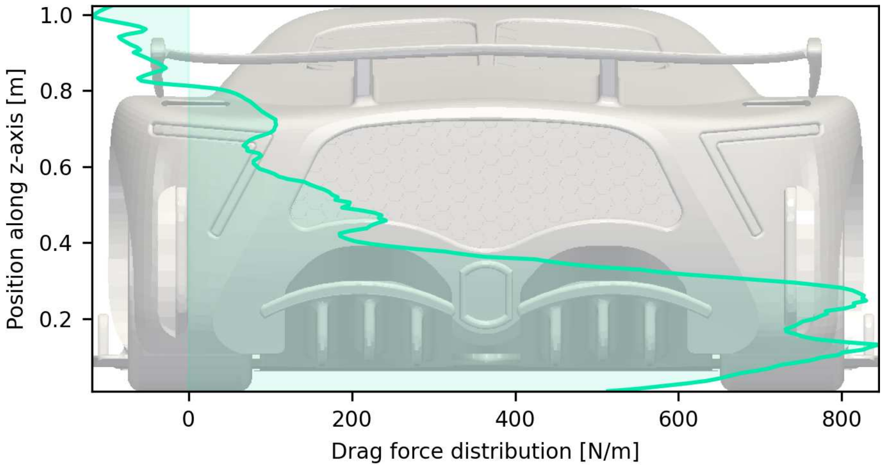

Figure 47: Drag force along z-axis

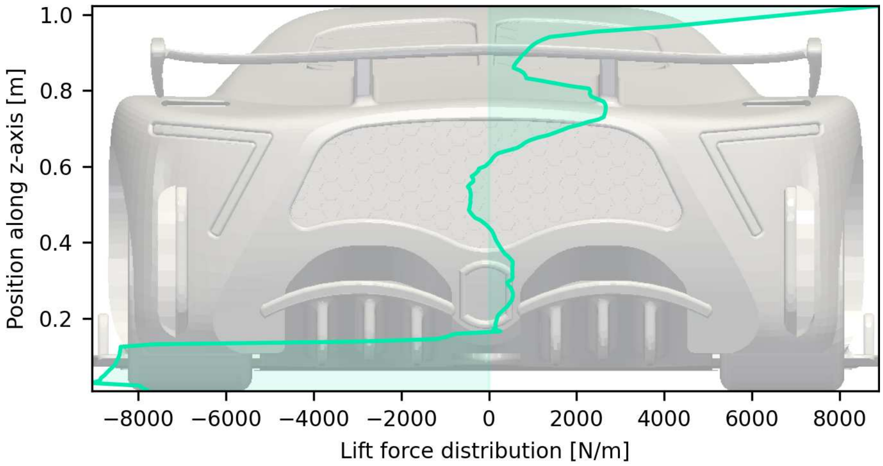

Figure 48: Lift force along z-axis

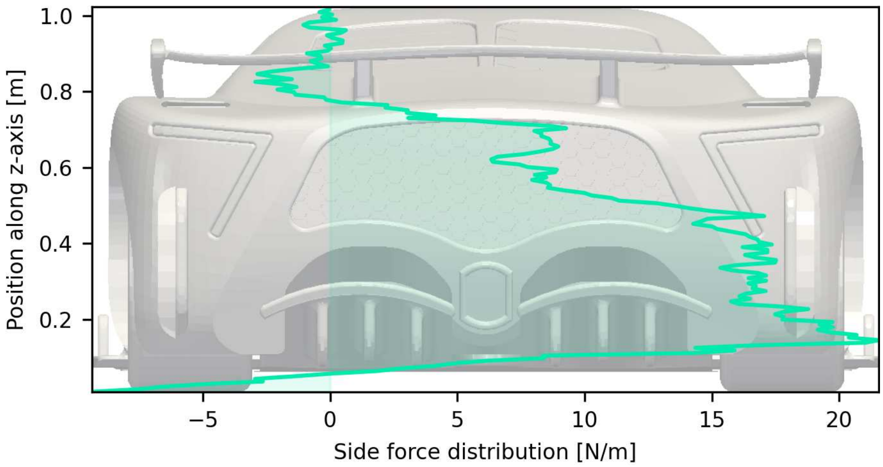

Figure 49: Side force along z-axis

Part forces

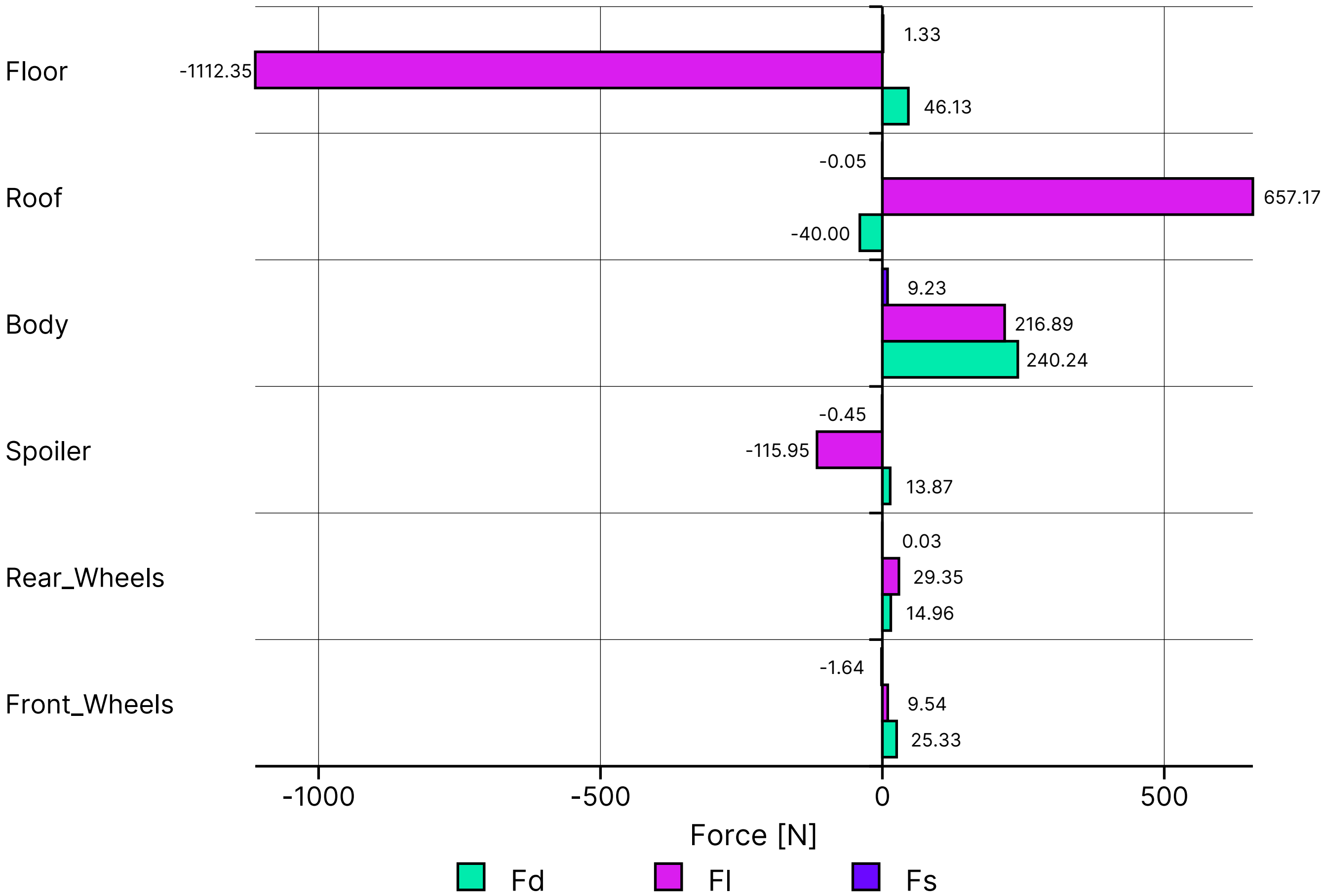

Figure 50: Aerodynamic forces by part, sorted by resultant force magnitude.

Drag force

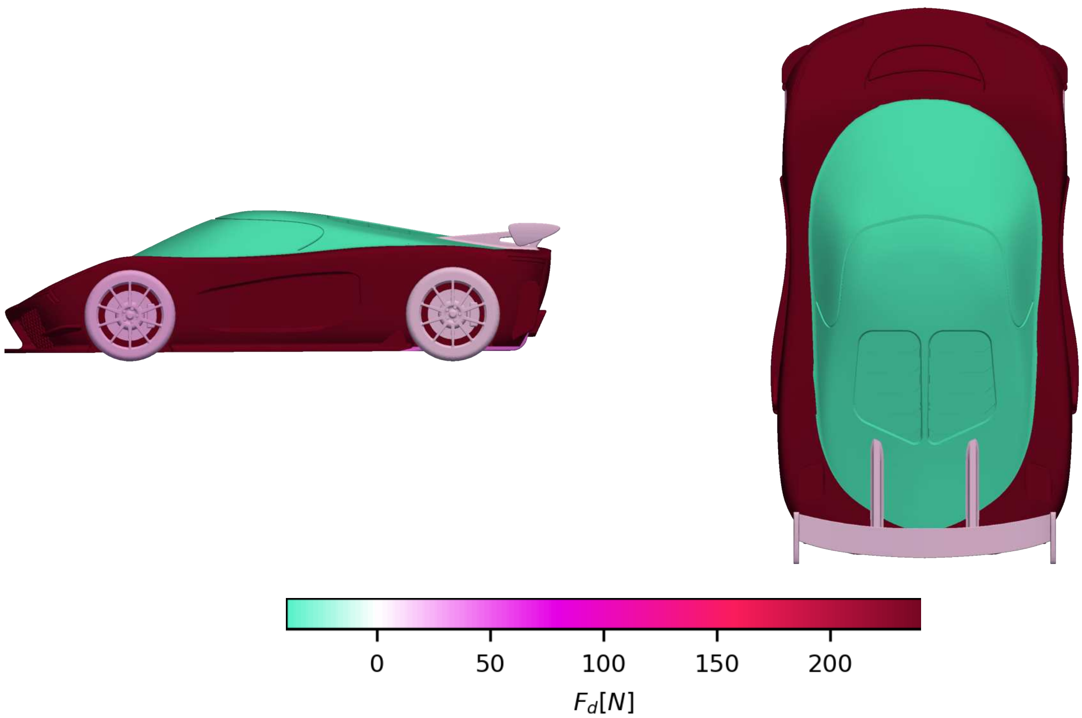

Figure 51: Drag force per part on 3D-model

Lift force

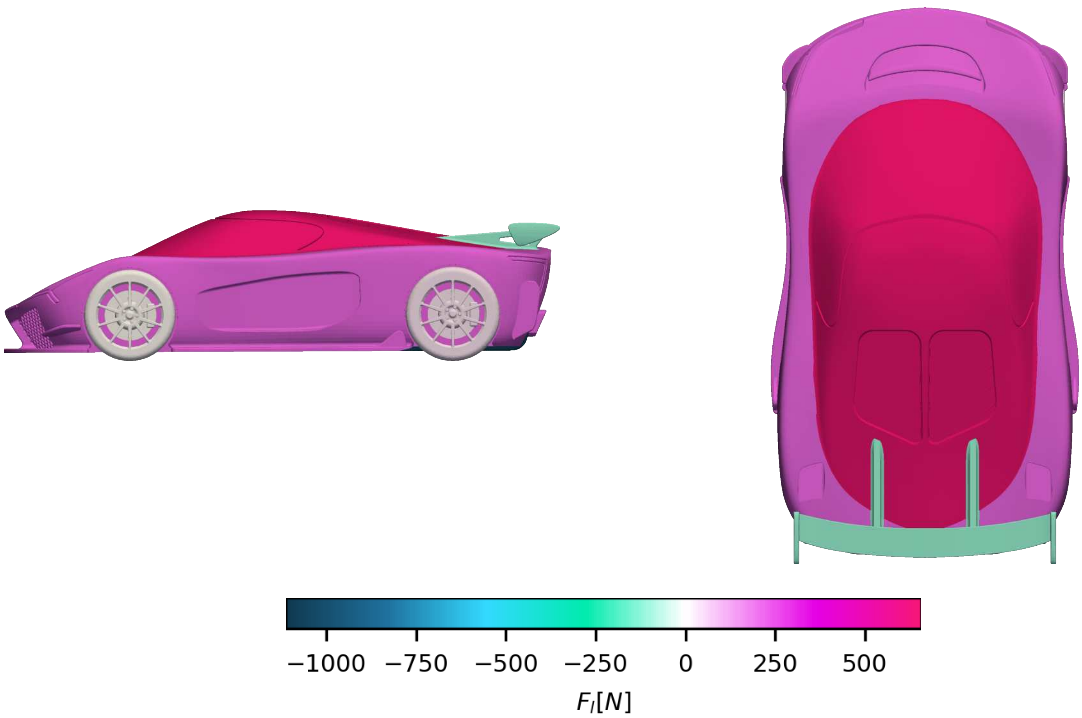

Figure 52: Lift force per part on 3D-model

Side force

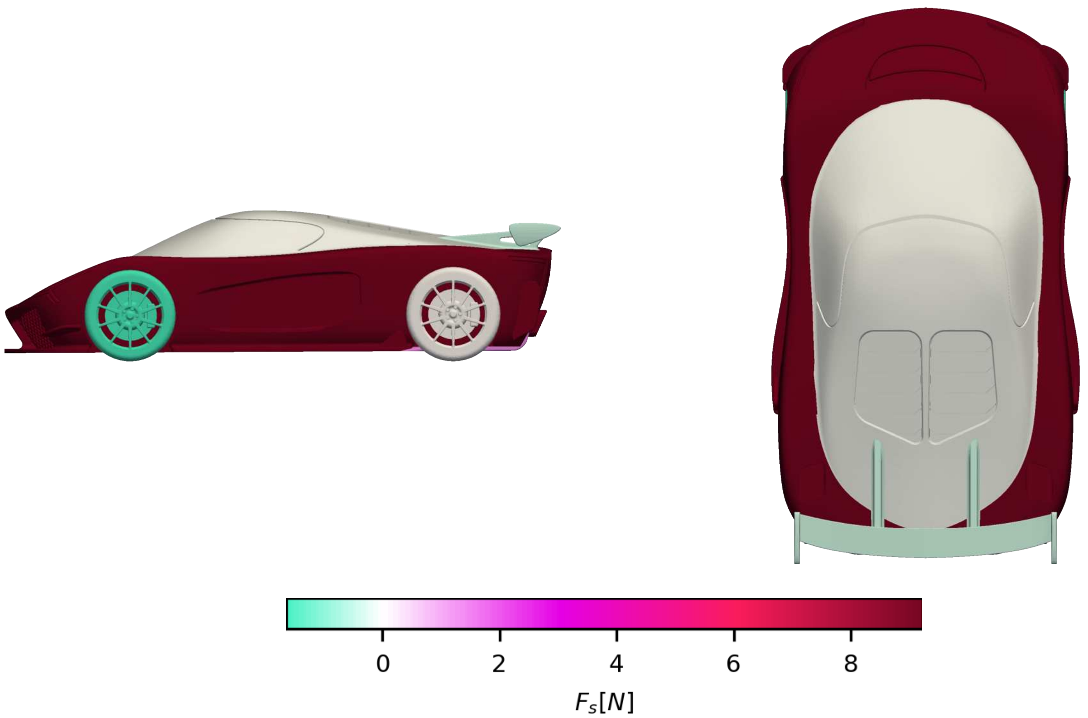

Figure 53: Side force per part on 3D-model

Simulation details Yaw-angle = 5.0°

Streamlines

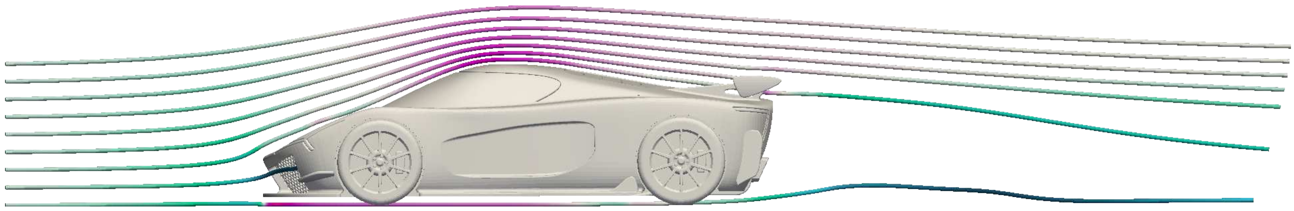

Figure 54: Streamlines left view

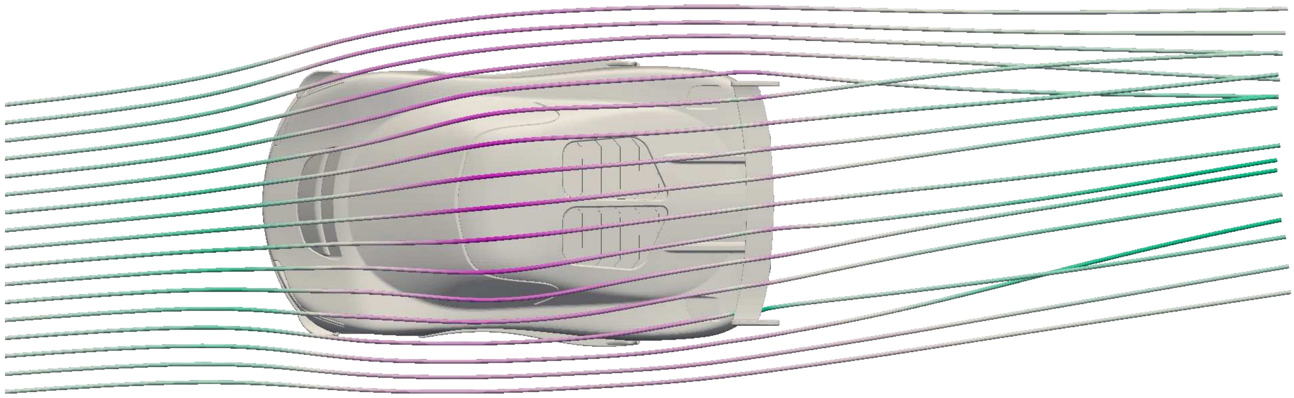

Figure 55: Streamlines top view

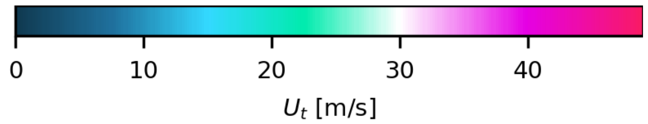

Pressure field

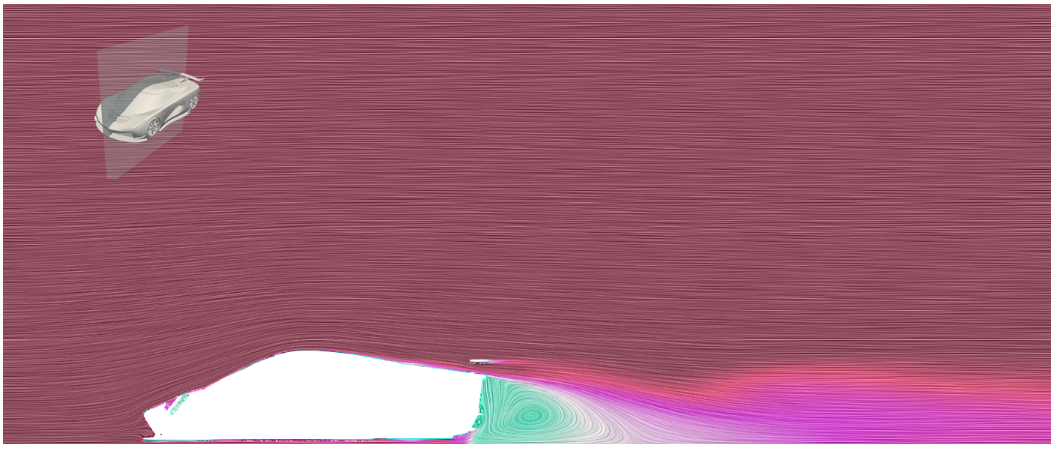

Figure 56: C_{pt} Total pressure coefficient in model centre XZ-plane

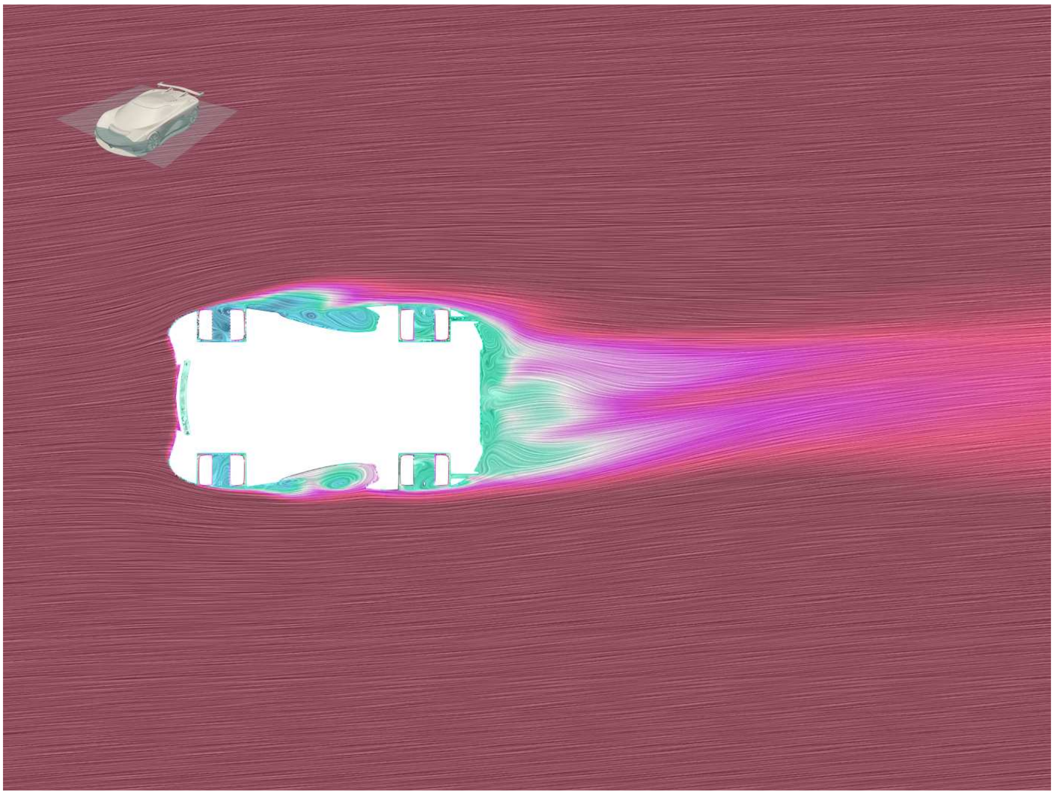

Figure 57: C_{pt} Total pressure coefficient in model centre XY-plane

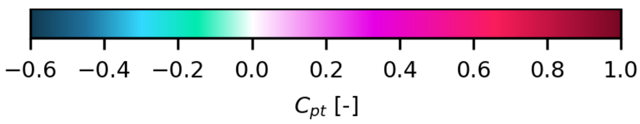

Surface pressure

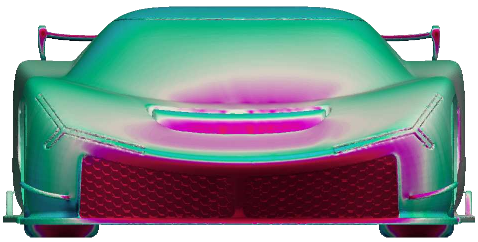

Figure 58: Surface pressure front view

Figure 59: Surface pressure back view

Figure 60: Surface pressure left view

Figure 61: Surface pressure right view

Figure 62: Surface pressure top view

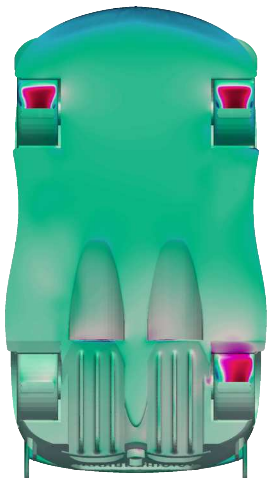

Figure 63: Surface pressure bottom view

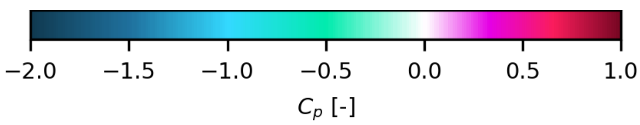

Wall shear stress

Figure 64: Wall shear stress front view

Figure 65: Wall shear stress back view

Figure 66: Wall shear stress left view

Figure 67: Wall shear stress right view

Figure 68: Wall shear stress top view

Figure 69: Wall shear stress bottom view

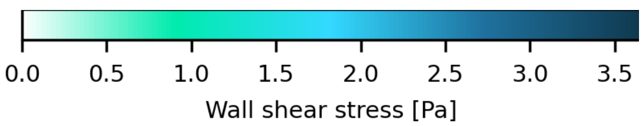

Drag pressure

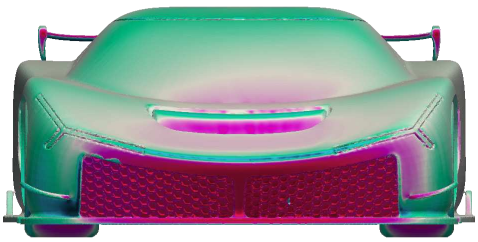

Figure 70: Drag pressure front view

Figure 71: Drag pressure back view

Figure 72: Drag pressure left view

Figure 73: Drag pressure right view

Figure 74: Drag pressure top view

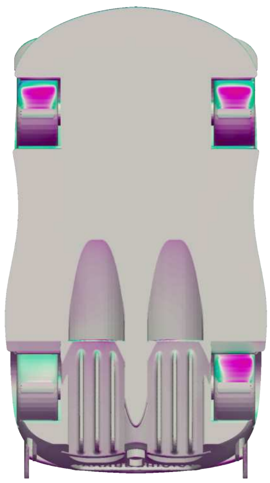

Figure 75: Drag pressure bottom view

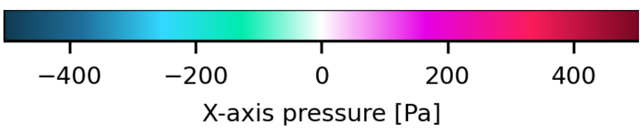

Recirculation zones


Figure 76: Recirculation zones front view

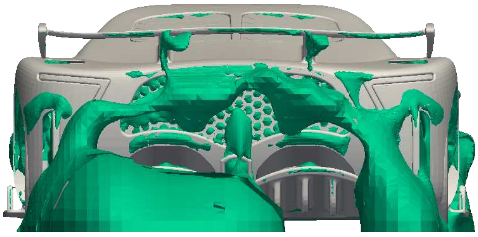
Figure 77: Recirculation zones back view


Figure 78: Recirculation zones left view


Figure 79: Recirculation zones right view


Figure 80: Recirculation zones top view


Figure 81: Recirculation zones bottom view

Wake development

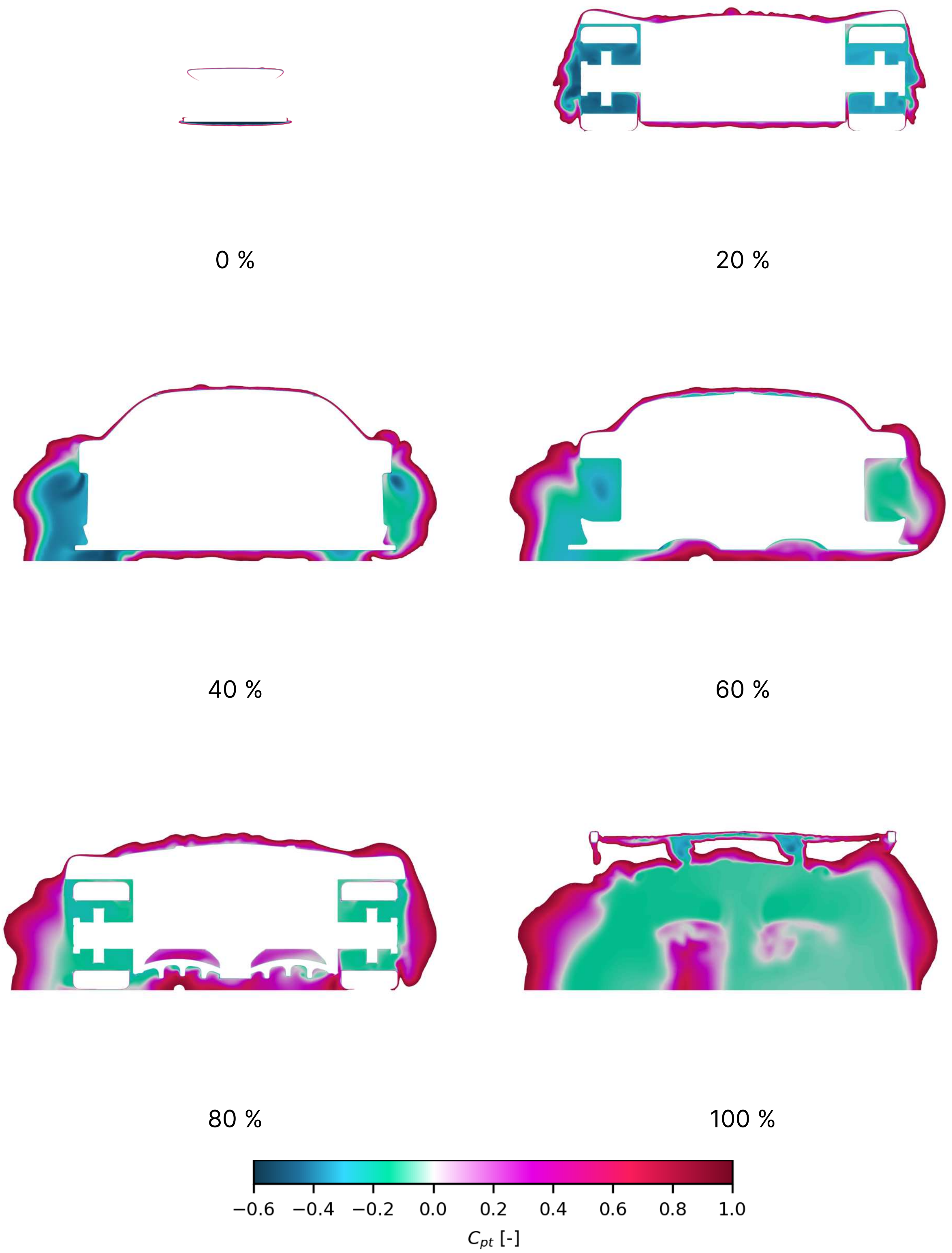

Figure 82: Wake development in the x-direction

Force distribution x-axis

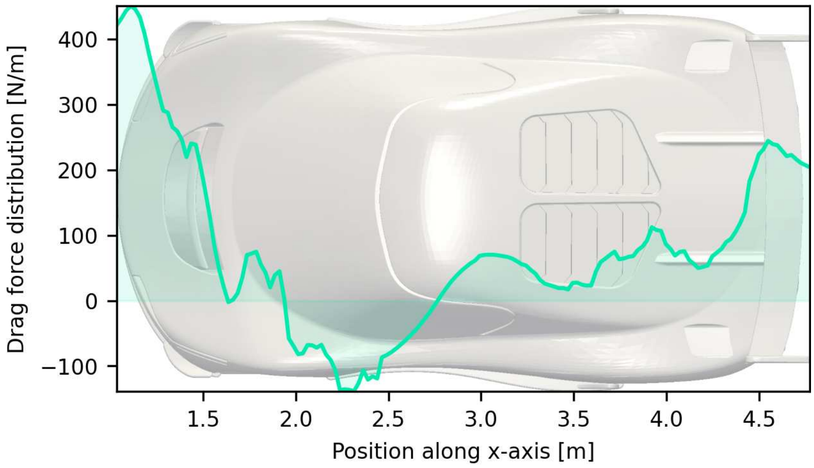

Figure 83: Drag force along x-axis

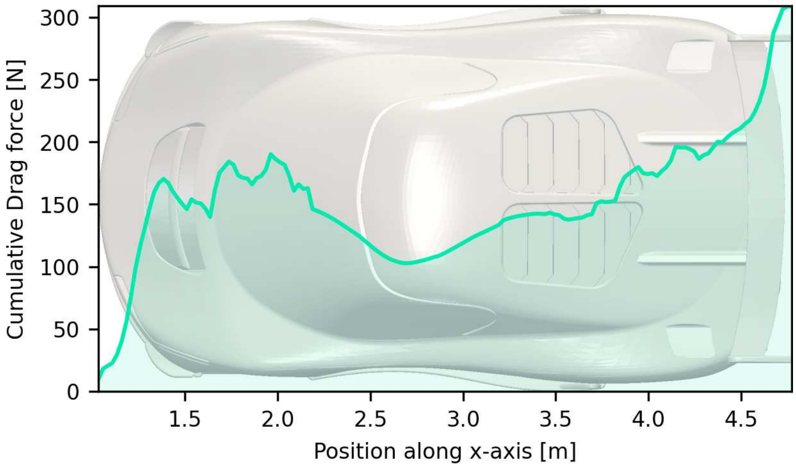

Figure 84: Cumulative drag force along x-axis

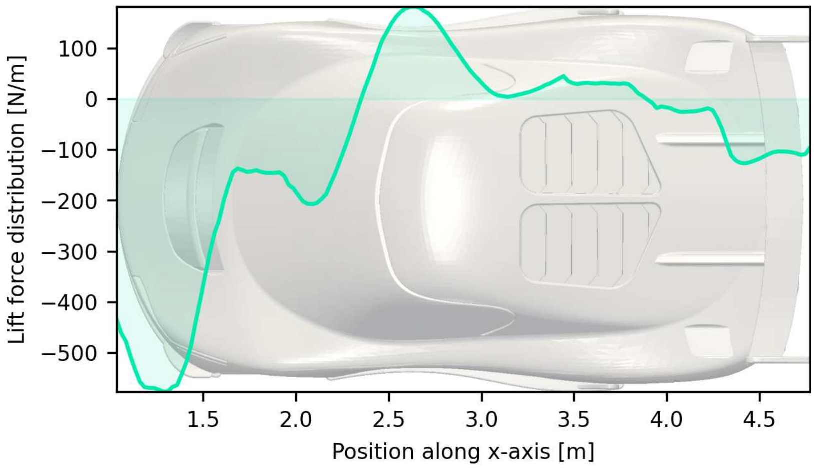

Figure 85: Lift force along x-axis

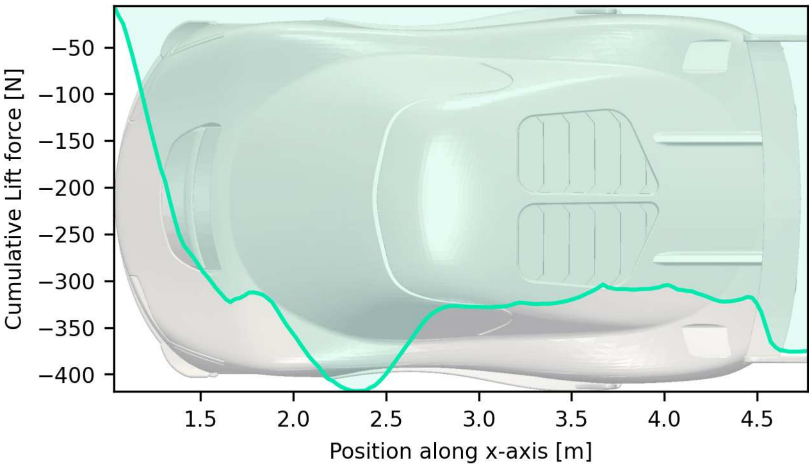

Figure 86: Cumulative lift force along x-axis

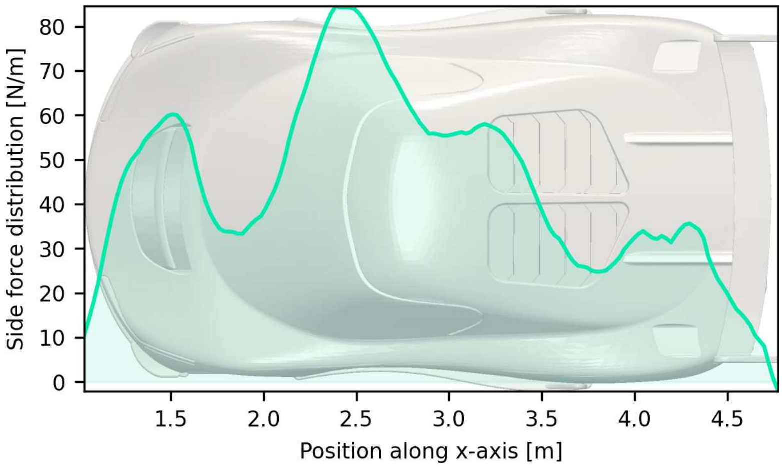

Figure 87: Side force along x-axis

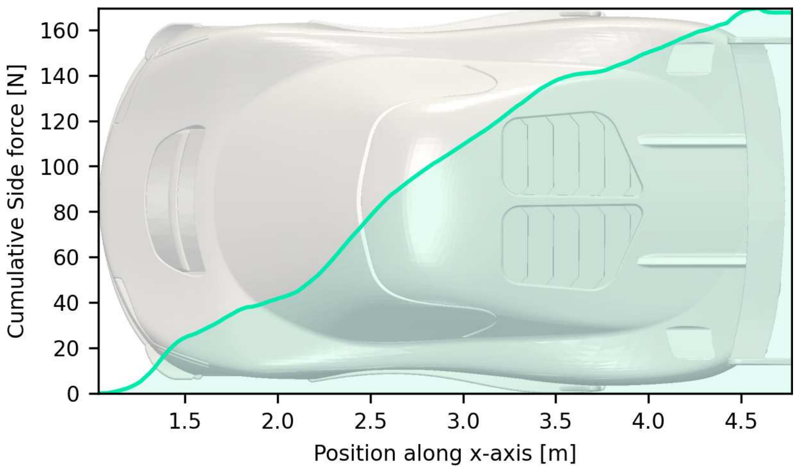

Figure 88: Cumulative side force along x-axis

Force distribution y-axis

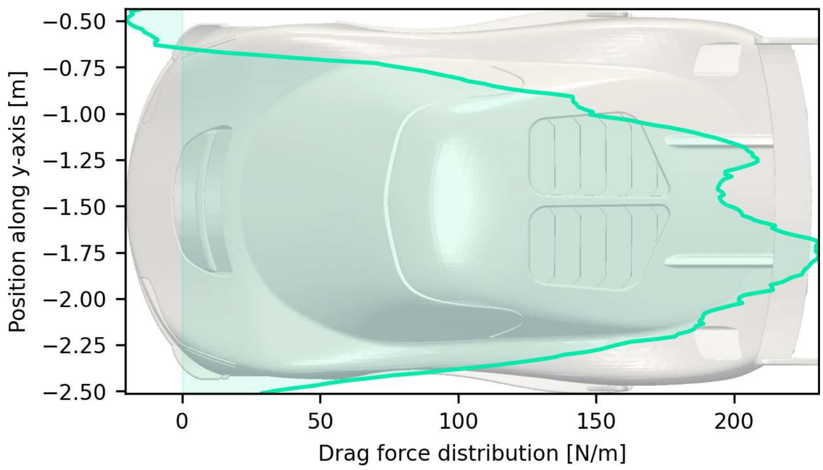

Figure 89: Drag force along y-axis

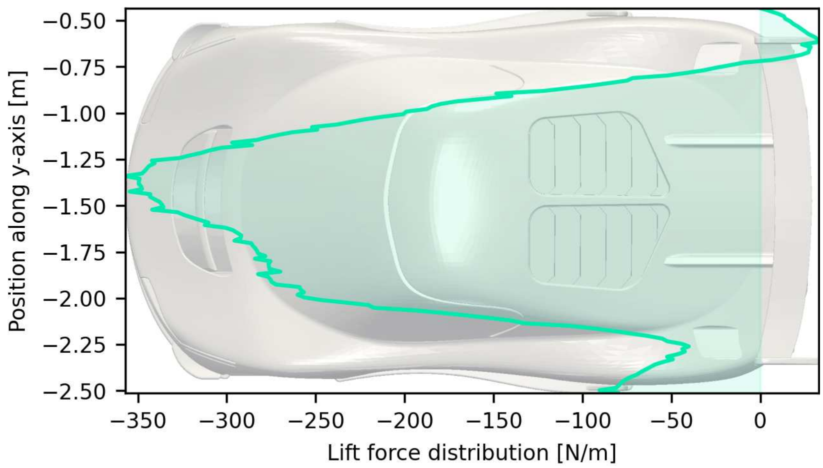

Figure 90: Lift force along y-axis

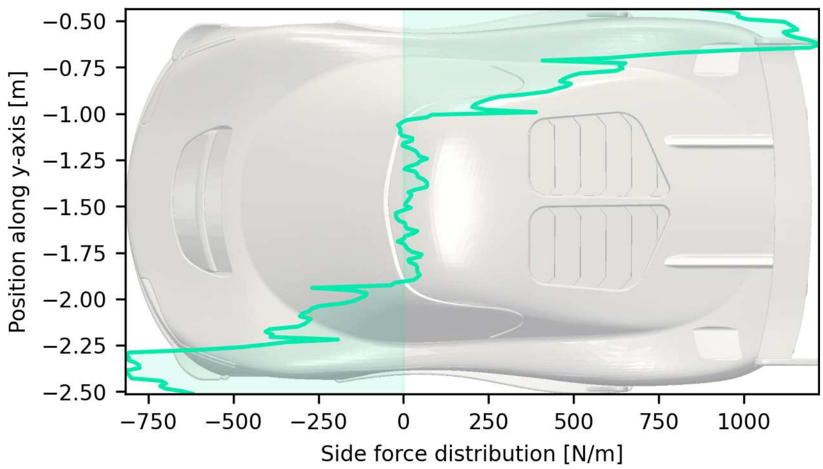

Figure 91: Side force along y-axis

Force distribution z-axis

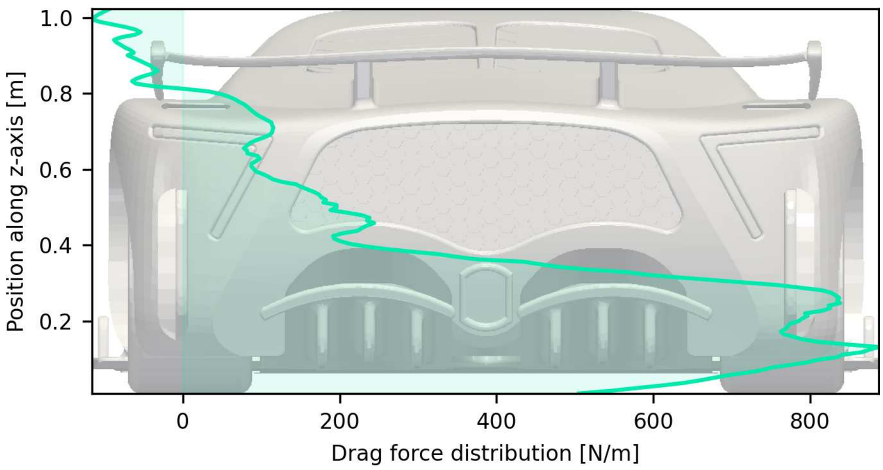

Figure 92: Drag force along z-axis

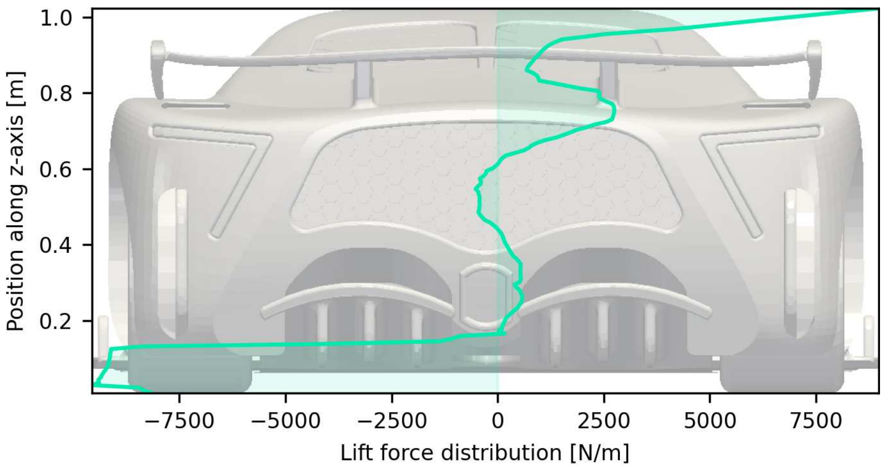

Figure 93: Lift force along z-axis

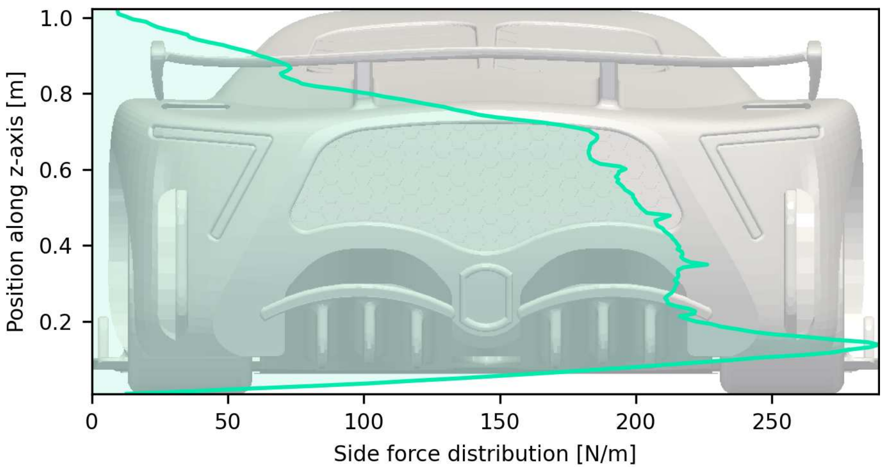

Figure 94: Side force along z-axis

Part forces

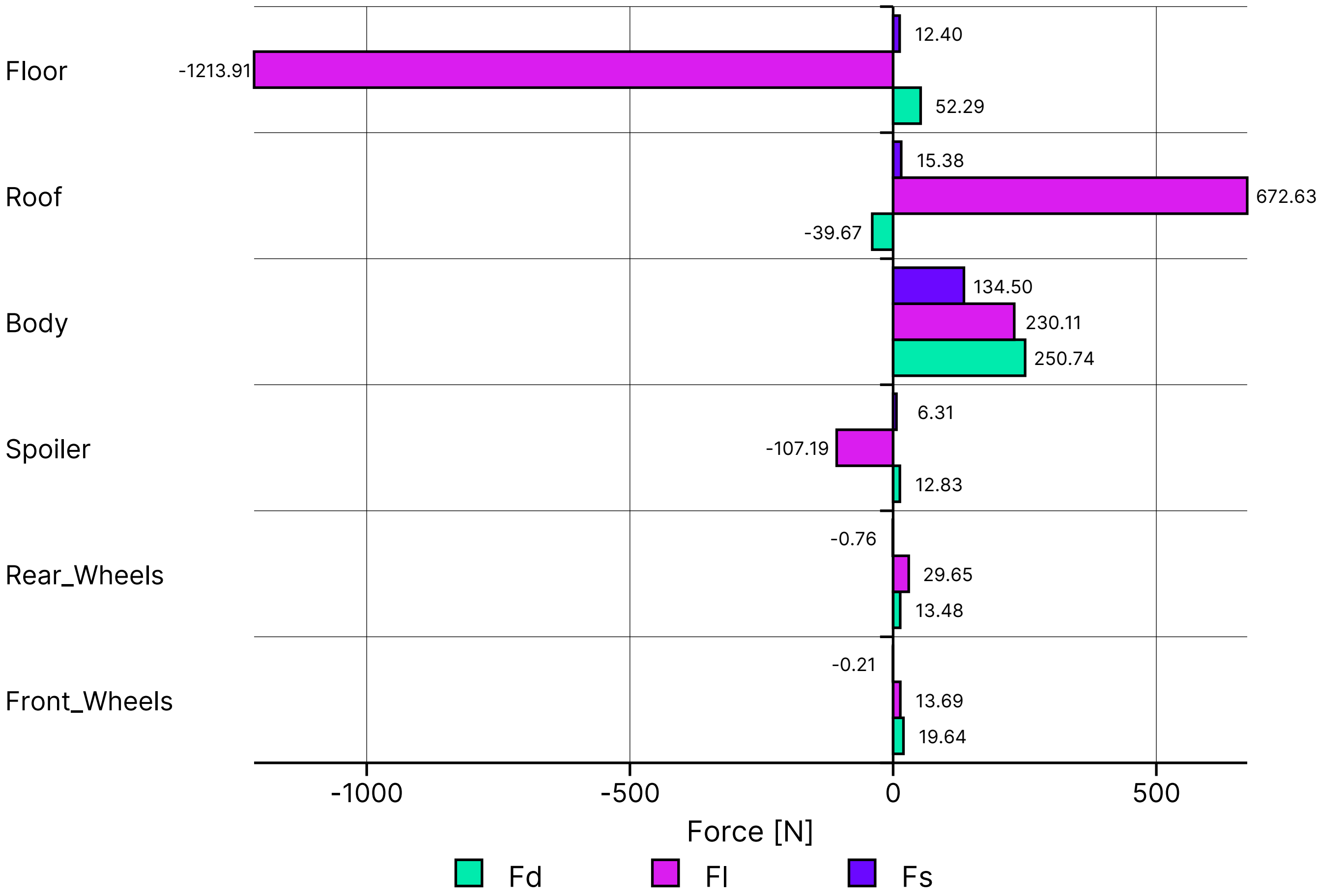

Figure 95: Aerodynamic forces by part, sorted by resultant force magnitude.

Drag force

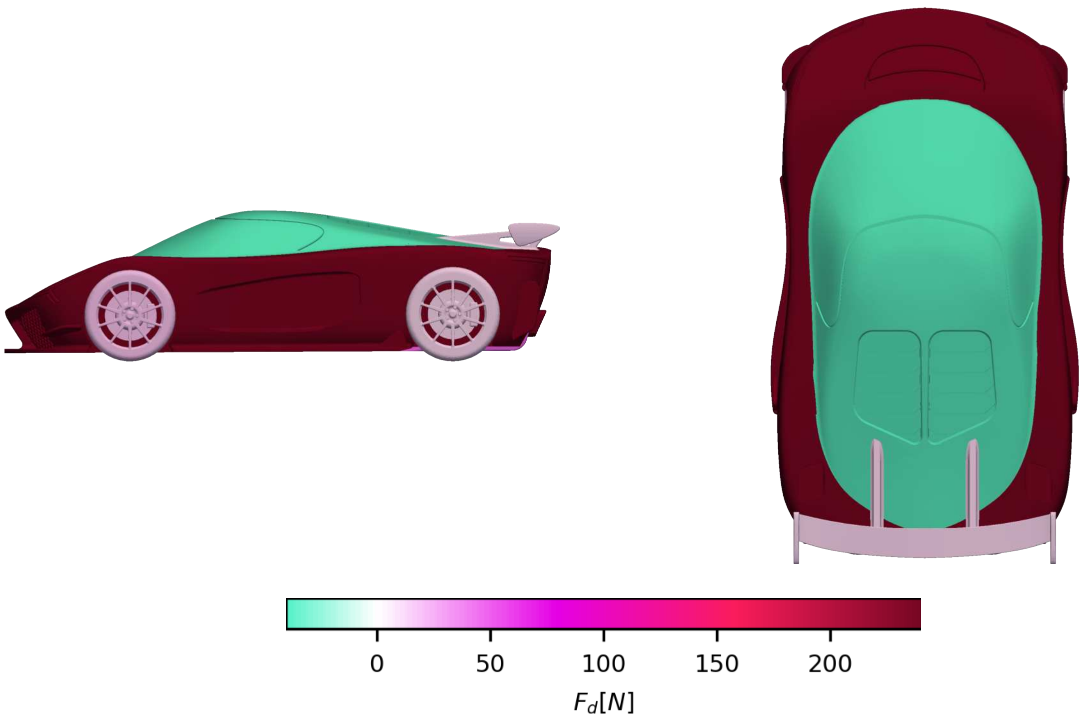

Figure 96: Drag force per part on 3D-model

Lift force

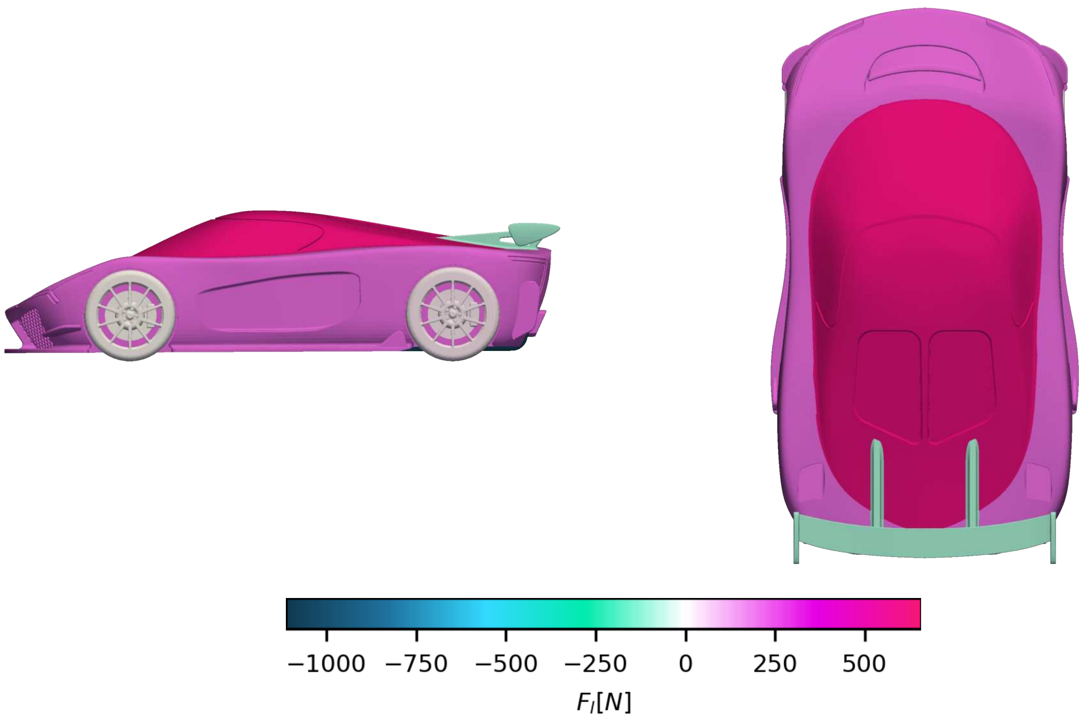

Figure 97: Lift force per part on 3D-model

Side force

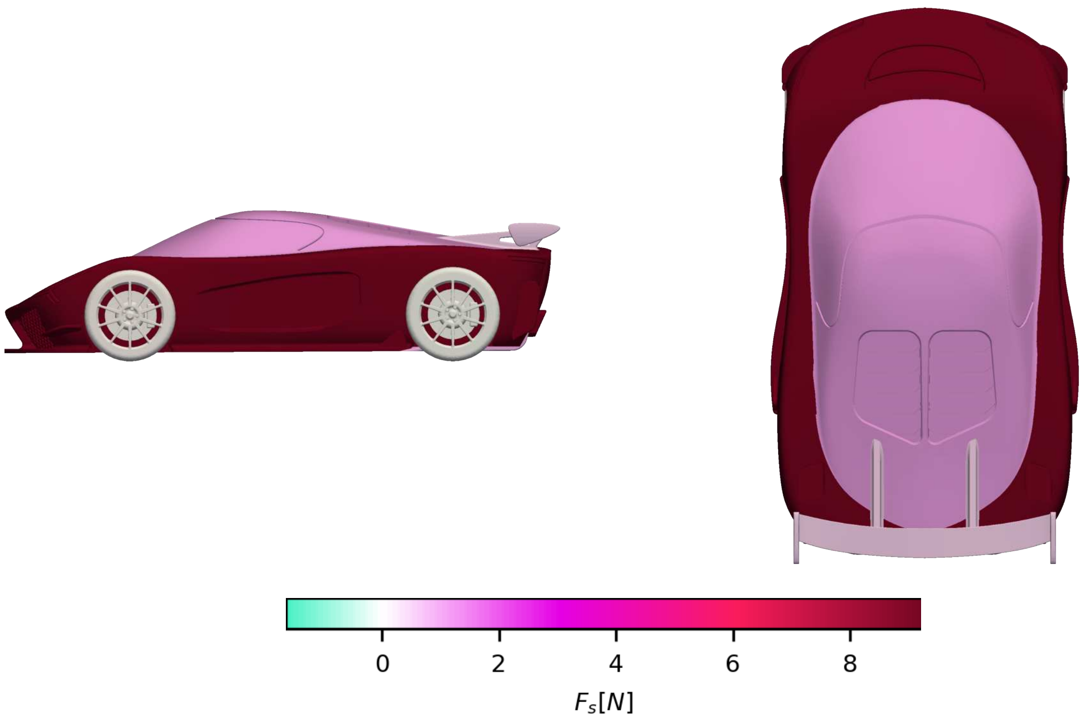

Figure 98: Side force per part on 3D-model

AEROCLOUD

Contacts

Nablaflow AS

Company Address	Sverdrups gate 27 4007 Stavanger
E-mail	info@nablaflow.io
Webpage	www.nablaflow.io

Appendix A Forces and moments per part

Yaw angle = 0.0°

Part	F_d [N]	F_s [N]	F_l [N]	M_r [Nm]	M_p [Nm]	M_y [Nm]
Roof	-39.999	-0.054	657.172	-971.261	-1915.260	-59.111
Rear_Wheels	14.961	0.032	29.348	-43.877	-113.216	21.570
Front_Wheels	25.334	-1.640	9.538	-13.163	-8.271	34.594
Body	240.238	9.228	216.887	-326.470	-647.147	388.821
Spoiler	13.869	-0.451	-115.951	173.301	542.506	18.520
Floor	46.128	1.333	-1112.347	1639.188	2577.093	73.373

Yaw angle = 5.0°

Part	F_d [N]	F_s [N]	F_l [N]	M_r [Nm]	M_p [Nm]	M_y [Nm]
Roof	-39.674	15.377	672.633	-991.394	-1964.352	-19.993
Rear_Wheels	13.484	-0.758	29.649	-54.361	-114.897	24.723
Front_Wheels	19.636	-0.210	13.687	-10.874	-17.943	28.213
Body	250.743	134.500	230.106	-365.905	-674.367	745.555
Spoiler	12.826	6.306	-107.186	148.055	501.964	47.832
Floor	52.288	12.399	-1213.910	1797.507	2941.848	123.563